Exploring haem-based alternatives for oxygen reduction catalysis in fuel cells—a status report of our first principles calculations

Exploring haem-based alternatives for oxygen reduction catalysis in fuel cells—a status report of our first principles calculations

E S Dy[1], **T A Roman**[1], **Y Kubota**[1,2], **K Miyamoto**[1] **and H Kasai**[1,3]

[1] Department of Precision Science and Technology and Applied Physics, Graduate School of Engineering, Osaka University, 2-1 Yamadaoka, Suita 565-0871, Japan
[2] Power Engineering Research and Development Center, Research and Development Department, Kansai Electric Power Co., Inc., Amagasaki, Hyogo 661-0974, Japan

E-mail: kasai@dyn.ap.eng.osaka-u.ac.jp

Abstract
For hydrogen fuel cells to become commercially viable, an alternative catalyst to platinum surfaces that is both efficient and affordable must be discovered. We consider haem and haem derivatives as potentials substitutes. In this paper, we discuss the oxygen reduction reaction on both the platinum surface and on haem. We then introduce our suggestions based on density-functional studies on how to improve haem's oxygen-reduction capabilities, which can be summarized as follows: inducing the singlet state, inducing side-on interaction, mimicking cytochrome c oxidase by adding a copper–imidazole complex, using platinum deposited on tin porphyrin instead of haem, and using oxomolybdenum porphyrin instead of haem. We shall focus on the last three methods because of their experimental practicability.

1. Introduction

Fuel cells are among the most promising alternative power generators of the future. Unlike boilers and internal combustion engines, they are not constrained by the efficiency limitations of the Carnot cycle. A key player in the field of fuel cells is the hydrogen-fuel polymer electrolyte fuel cell (PEFC), of which a schematic diagram is shown in figure 1. To make it work, hydrogen is first directed to the fuel cell's anode, which dissociates the incoming gas molecules and strips the atoms of their electrons. Platinum (Pt) has been a popular catalyst choice for this reaction, as experiment and theory agree that the reaction may proceed effortlessly, i.e., the energy barrier for the dissociation can be very low. The protons then diffuse along the surface of the anode catalyst, which is another relatively easy process [1, 2]. Meanwhile, the load is powered by

---

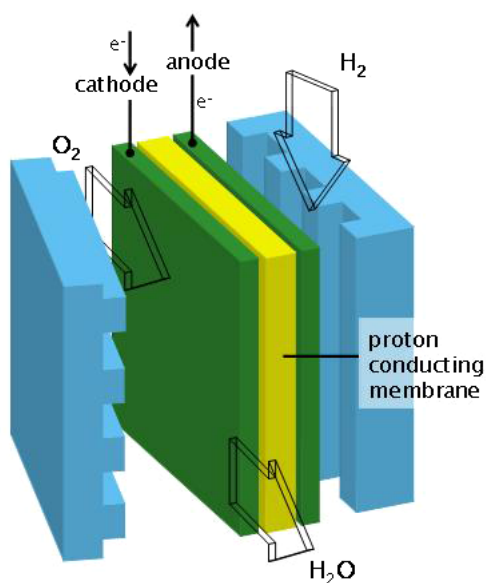[3] Author to whom any correspondence should be addressed.

Figure 1. Schematic diagram of a fuel cell.
(This figure is in colour only in the electronic version)

the produced electron current, and the protons diffuse through a membrane made of a material specific to proton conduction, e.g. the polymer Nafion. At the fuel cell's cathode, oxygen combines with the protons to form water as it undergoes reduction. This completes the fuel cell's *catalytic combustion* routine for generating electricity.

Clearly, a macro-scale understanding of how the fuel cell should work is not a formidable task. However, realizing one fit for mass production is. For Pt-based fuel cells, for example, there are performance issues that need to be addressed, such as carbon monoxide poisoning of the electrode catalysts. There are long-term durability difficulties that need to be overcome as well. But ultimately, the biggest obstacle to the widespread use of hydrogen fuel cells is cost. While fuel cells give excellent value for money in terms of energy–fuel-consumption efficiency, current prototypes are still beyond the purchasing power of the average consumer primarily due to the cost of the precious metal Pt, which has been the preferred material for anodes and cathodes across most types of fuel cell. This has sparked the search for alternative catalysts, especially for the oxygen reduction reaction (ORR) occurring at the fuel cell cathode. While Pt is a good electrical conductor, resistant to corrosion and high temperature, and the most catalytically active, the over-potential and reaction rate for oxygen reduction on Pt is still relatively poor when compared to hydrogen oxidation. This means that the conversion of O_2 to water (reduction) at the cathode remains the bottleneck for the flow of electrical current for a hydrogen-fuel PEFC.

2. O_2 reduction on platinum

At present, platinum surfaces are considered the model electrode catalysts for fuel cells. The reduction of O_2 on Pt surfaces (and metal surfaces in general) can be simplified [3] as shown in figure 2. K_1 to K_5 represent the reaction rate of each process. Ideally, either K_1 or both K_2 and K_3 should be very high while K_4 and K_5 should be zero—this is called a four-electron
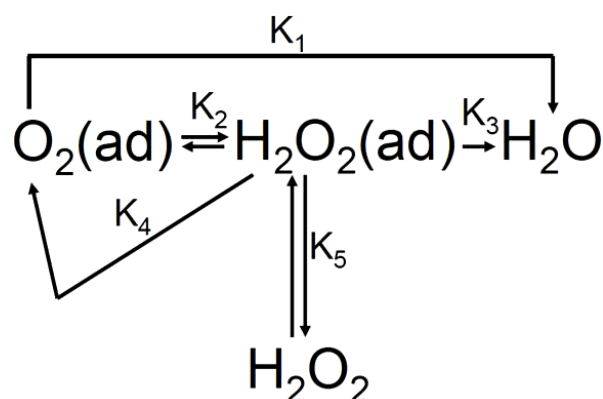
Figure 2. Reaction paths for the reduction of O_2 adsorbed on metal surface.

reduction process. On the other hand, if K_1 and K_3 are almost zero and K_2 and K_5 are high, a two-electron reduction process predominates and hydrogen peroxide (H_2O_2) can diffuse into the environment. This degrades the performance of a fuel cell in terms of lower electromotive potential generated and potential damage to the proton transfer membrane.

The reduction of O_2 on Pt is a complex subject affected by factors such as crystal face indices, oxygen coverage, intermediates (e.g., –O, –OOH, –OH) formed, vacancies, impurities, environment (e.g. electrolytic used), temperature and pressure. Extensive reviews have been done by Markovic and Ross [4, 5] and also by Adzic [6] and they will not be covered in depth in this paper.

Low-pressure experiments (10^{-6} Torr, O_2) have shown that O_2 molecules undergo dissociative adsorption on a clean Pt(111) surface at temperatures typical of PEFC operation (80 °C). This is in contrast to low temperatures (−153 °C and below), where molecular adsorption is preferred; the O_2 molecules then dissociate into atoms when heated. At temperatures of around 800 °C, a stable oxide is formed, but the oxygen eventually desorbs at 927 °C [7]. Of note is that the formation of surface oxides leads to reconstruction of the Pt surface. Formation of stable oxides (stable up to <726 °C) has been shown to poison the catalytic activity of Pt(100) for CO oxidation [8]. While these studies are not directly about the reduction of oxygen into water in a humidified Nafion environment, they inform us of the possible interactions that oxygen may undergo with the platinum surface.

An *ab initio* study by Eichler and Hafner [9] splits the adsorption process into three phases: the physisorbed molecular O_2, the chemisorbed molecular O_2, and chemisorbed dissociated atomic O on Pt(111). Their study shows that the chemisorbed O_2 is a paramagnetic superoxo (O_2^-) species at the bridge site and a diamagnetic peroxo (O_2^{2-}) species when adsorbed at the three-fold hollow site. Our group, on the other hand, compared the dissociative adsorption of O_2 on two types of Pt surfaces, namely, Pt(001) and Pt(111), by density-functional calculations [10]. Of the several factors that may govern O_2 dissociative adsorption, we concentrated on the static effect of surface structure. (Larger distances between Pt atoms exist in the hollow sites of Pt(001) as compared to Pt(111).) The calculated potential barrier (E_{ac}) for O_2/Pt(001) ($E_{ac} = 1.2$ eV) is smaller than that for O_2/Pt(111) ($E_{ac} = 1.7$ eV). This indicates that the O_2 dissociative adsorption occurs much more easily on the Pt(001) surface than on the Pt(111) surface, which is in good agreement with experimental observations [11–13].

In liquid electrolyte solutions, more complex ORR situations occur due to the competitive adsorption of the electrolyte's anionic species on platinum. Rotating disc electrode (RDE)

studies show that the relative activity of platinum catalysts varies with crystal face in the order of (111) $\ll$ (100) < (110) for sulfuric acid, (100) < (110) $\approx$ (111) for perchloric acid, and (100) < (110) < (111) for KOH. Sulfuric acid was shown to have the strongest deactivating effect [14].   However, fluorosulfonic acid side-chains of polymer electrolyte membranes (e.g. Nafion) used in PEFCs was shown to not interfere with the reaction kinetics [15–17].

Recent studies have focused on designing new experimental set-ups for assessing the activity of catalysts with Nafion in the absence of liquid electrolytes and at temperature and humidity conditions which will simulate the PEFC environment more accurately [18, 19]. In one such study, Pt(111) was reported to be twice as active as Pt(100), although details of the kinetics or activation energies have not been published at this time [18].

Density-functional calculations, particularly those from the groups of Anderson [20, 21] and Norskov [22], consider the effects of electromotive potentials on the ORR. According to the study of Norskov *et al* [22], OH and O are said to adsorb more stably on Pt surfaces as the potential (due to the presence of an external load) approaches equilibrium. In the process, the transfer of H^+ and electrons to these species becomes more difficult and, in effect, determines the rate of reaction. They popularized what is now popularly known as the 'volcano' relationship between the rate of ORR versus the O and OH binding energy on various metals. Pt(111), which sits on top of the activity volcano curve, has binding energies of 1.05 and 1.57 eV for OH and O respectively. It would be thus also useful to determine the OH and O binding energy of our computationally designed catalysts and fit it into the volcano curve to predict its activity. Of note is their studies which suggest that, at high (0.5) O_2 coverage, molecular adsorption of O_2 and reduction via a peroxide mechanism is preferred (at 298 K).

3. O_2 reduction on haem

In contrast to the present platinum-based technology, nature has its own way of reducing dioxygen without the need for expensive rare metals. With this in mind, our group suggested using haem components [23] for use as fuel cell ORR catalysts.   Our group has also performed density functional calculations on a haem-based Fe–porphyrin (FePor) nanowire, where the adjacent porphyrin macrocycles are linked in parallel, and the result is electrically conductive [24]. Electronic conductivity is a necessary property for fuel cell electrodes to move electrons efficiently. Thus haem-based materials are potential electrode surfaces from the perspective that they can both conduct electricity and reduce oxygen.

Haem occurs in nature as the active site of a variety of biological proteins that interact with O_2. Haemoglobin is used to transport oxygen; myoglobin is used for oxygen transport and storage; cytochrome c oxidase and cytochrome P 450 are used to reduce O_2. Haem (figure 3) is composed of an iron (Fe) metal centre, a porphyrin ring (Por) and some side chains. As shown in the inset of figure 3, the Por is a planar aromatic macrocycle made of hydrogen, carbon and nitrogen atoms. The Por ring has a net charge of 2− and bonds to the central Fe atom through the four nitrogens. The central Fe atom is commonly found in the 2+ and 3+ oxidation states.

Due to its biological importance, the reaction of O_2 and haem has been the subject of many theoretical and experimental studies [25–39]. Many of these density-functional studies are performed in vacuum. This is justifiable because, while biological molecules naturally exist in aqueous solution, the haem active sites are enclosed within hydrophobic portions of proteins. The current understanding based on the above literature relevant to our fuel cell ORR concerns can be summarized as follows:

(1) X-ray diffraction and density-functional theory (DFT) calculations show that O_2 normally binds to the central Fe atom via a side-on configuration at an Fe–O–O angle of 122°–130°.
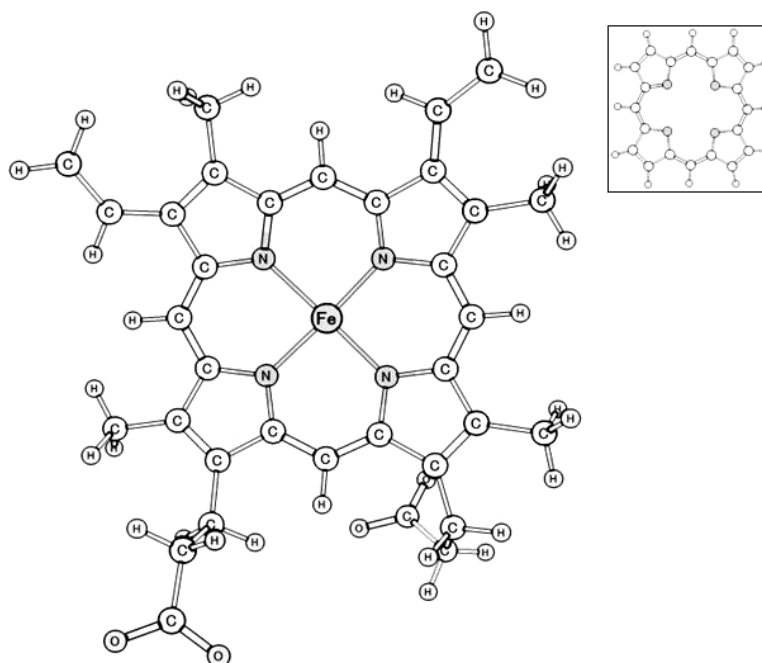
Figure 3. Haem is composed of an iron (Fe) metal centre surrounded by a porphyrin macrocycle (also shown in the upper right inset) with some side chains.

O_2 pulls the Fe away from the porphyrin plane [31–33]. Electron transfer occurs from Fe to the O_2 in the process. The spin state of Fe changes depending on the ligands attached. FePor is a triplet and FePor–O_2 is a singlet based on density-functional studies [33].

(2) A variety of mechanisms for the reduction of O_2 on FePor-based molecules has been deduced from Raman spectroscopy, extended x-ray absorption fine-structure (EXAFS) analysis and DFT calculations. Intermediates including the formation of ferric–superoxo, ferric–peroxo, ferric–hydroxy and ferryl–oxo complexes have been proposed [34–36].

(3) CO can poison FePor. Kinetics studies show that the binding affinity of CO on haem is higher than that of O_2 by a factor of 20 000. In haemoglobin and myoglobin, this poisoning effect is minimized by the protein environment to a CO/O_2 binding affinity factor of only 25–270 [37]. The binding energy of O_2 on FePor, computed by density functional theory, was found to be 0.09 eV while that of CO was 0.27 eV [33]. CO binds vertically to the Fe and back donation of Fe d electrons to the vacant anti-bonding orbitals of CO occurs, consequently enhancing the Fe–CO bond strength. The O_2 in myoglobin is thought to be stabilized by a distal histidine from the protein environment through hydrogen bonding to make it competitive with CO. This is supported by both experimental studies on half-saturation pressures of $O_2(p_{1/2}^{O2})$ on haem and their synthetic analogues [34] as well as by DFT calculations [38]. Another contributing factor is that CO is disfavoured by steric effects in the protein as CO requires linear Fe–C–O geometry on FePor, whereas Fe–O–O is bent as mentioned earlier. Collman *et al* have synthesized haem analogues with hydrocarbon groups serving as caps over the porphyrin plane. They demonstrated strong correlation between the porphyrin-to-cap distance and M $(p_{1/2}^{O2}/p_{1/2}^{CO})$—with M reaching as high as 1.2×10^5 [39].
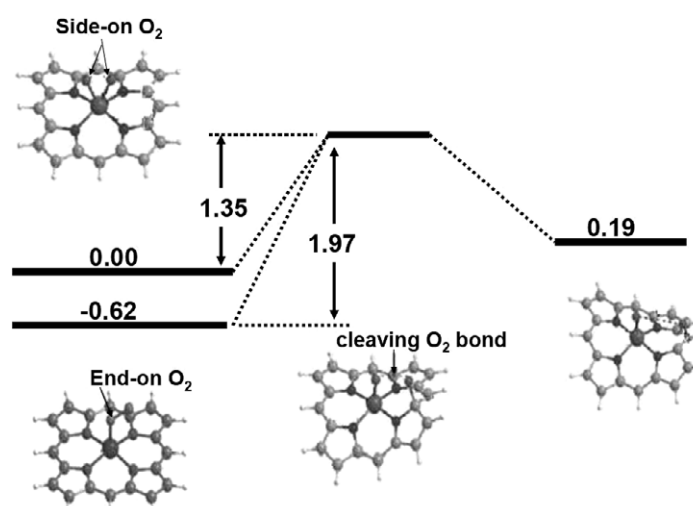
Figure 4. The bond dissociation barrier of side-on and end-on O_2 on Fe–Por are 1.35 eV and 1.97 eV respectively.

(4) The activation barrier for O_2 bond dissociation on FePor at 1.97 eV [23] is higher compared to Pt.

4. Haem-based alternatives for fuel cell cathode catalysts

Studies have demonstrated that haem-like compounds adsorbed on or bonded to a carbon support are catalytically active for O_2 reduction [40–43]. Yet none of their prototypes' performance rivals that of the Pt catalyst in terms of stability and efficiency. Logically, the next course of action would be to determine how we can improve on the ORR capabilities of haem-based catalysts. We have proposed several ways to achieve these based on our density-functional calculations.

We consider finding materials with O–O bond dissociation activation barriers that fall near the range between that calculated for Pt(111) and Pt(001) as a first step towards finding alternative ORR catalysts. Our early studies involve utilizing physical techniques, such as inducing the side-on interaction of O_2 with FePor [44], to achieve this. The O–O bond of the side-on adsorbed O_2 on FePor–O_2 is relatively weak (1.42 Å versus 1.2 Å for O_2 gas in vacuum), and the side-on O–O bond dissociation barrier (1.35 eV) on FePor is energetically comparable to that of the well-known platinum catalyst as shown in figure 4. We propose impinging O_2 as oriented molecular beams [45–47] aligned to the haem surface to verify our suggestion.

Another proposal involves magnetizing (Im)FePor–O_2 (FePor–O_2 with an imidazole) to the triplet state [48] as shown in figure 5. The addition of an imidazole (Im) opposite O_2 on FePor while, at the same time, inducing the triplet state also lowers the activation energy for the dissociation of O–O on haem. The imidazole was said to enhance spin polarization on the Fe and weakening of O–O bond in the triplet state. By inducing the triplet state, the activation barrier for O–O dissociation barrier is lowered to 1.19 eV. We suggest that a strong external magnetic field be applied for this purpose.

While these physical techniques are academically interesting, inducing the triplet state and the side-on interaction are challenging tasks that have yet to be addressed. Consequently, in
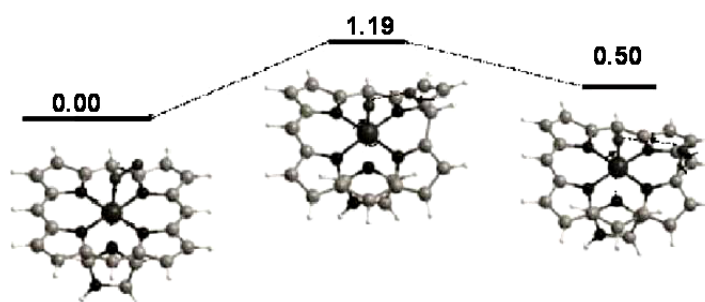
Figure 5. Adding an imidazole ligand below the Fe and inducing the triplet state reduced the bond dissociation barrier of O_2 on Fe–Por to 1.19 eV.
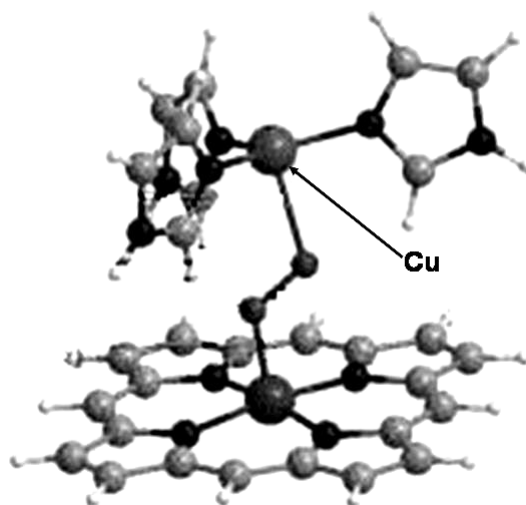

Figure 6. The active binuclear centre of CcO. The $Cu(Im)_3$ binds to the distal oxygen atom of FePor–O_2.

our more recent works, we focus on designing new materials. We would like to focus on the methods below due to their readiness for experimental verification.

4.1. Cytochrome C oxidase mimic

Cytochrome c oxidase (CcO) is an oxidase enzyme that catalyses cell respiration in virtually all aerobic organisms [49]. The active site of CcO is a haem–copper binuclear centre, in which a Cu complex affects the O_2–haem binding and the O–O bond reductive cleavage [49]. The catalytic activity of CcO in biological systems motivated us to evaluate whether a Cu complex would accelerate O_2 dissociation on FePor.

We consider FePor and copper–(imidazole)$_3$ [$Cu(Im)_3$] as the representative of the active binuclear centre of CcO (figure 6) [50]. The Cu binds to the distal oxygen atom of FePor–O_2 and, in effect, weakens the O–O bond. This is manifested by an increase in O=O bond length (1.32 Å for FeP–O_2 versus 1.38 Å for FeP–O_2–$Cu(Im)_3$) and a decrease in O=O stretching frequency (1211–1082 cm^{-1}). We find that the $Cu(Im)_3$ weakens the O–O bond primarily by electron transfer to the oxygen atoms. In the FeP–O_2, the charges of the Fe and O_2 are 0.964
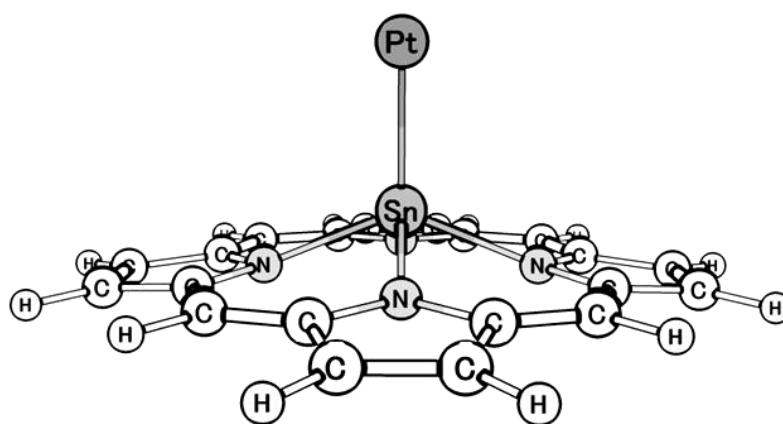
Figure 7. Relaxed geometry of platinum deposited on the surface of tin porphyrin.

and -0.229, respectively. In the FeP–O_2–[Cu(Im)$_3$], on the other hand, the charges of the Fe and O_2 are 1.531 and $-0.717/-0.877$, respectively. O_2 bond weakening leads to easier O–O bond dissociation while the negative charge transfer to O makes it more reactive to H$^+$; both suggest ORR catalysis.

While we have yet to comple the reaction path for ORR on a CcO (to form the final product water), experimental studies [51] have already shown that cytochrome c oxidase mimics can indeed be synthesized to perform an ORR at high turnover rates. However, the experiments involved were intended to enable us to understand the mechanism of the ORR of biological CcO and not performed to simulate PEFC applications.
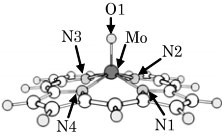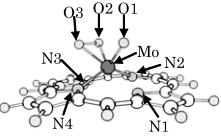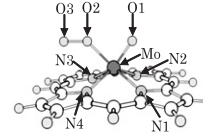
4.2. Depositing platinum on tin porphyrin or germanium porphyrin

Our idea was inspired by research which can be classified into two groups: first, studies that show that SnPor and GePor can deposit metals—such as iron (Fe), magnesium (Mg), rhenium (Re) and cobalt (Co)—on its surface by forming Ge–metal or Sn–metal bonds [52–57]; and, second, studies that demonstrate photocatalytic properties of tin porphyrins with Pt ions in solution. The reactions catalysed include the reduction of protons into hydrogen gas with ascorbic acid as electron donors and the self-assembly of Pt nanoparticles [58–60].

From these previous works, we consider depositing Pt directly on the SnPor surface as a way to minimize the Pt load in catalysts [61]. Our calculations show that Pt can bond strongly on SnPor. Dispersing platinum atoms on a porphyrin surface will—we believe—enhance their performance. The reasons for our belief are as follows: the top platinum metal (shown in figure 7) has minimal steric hindrances for incoming molecules compared to metals in surfaces or porphyrins; the presence of a porphyrin chromophore can trap light energy, possibly assisting the catalytic processes; and the perturbation on the electronic structure of Pt by the SnPor, as our calculations indicate [61], enhances its catalytic properties. The binding energy of platinum on SnPor was 3.13 eV, and the HOMO (highest occupied molecular orbital) and near-HOMO electrons (frontier electrons) correspond primarily to the valence d electrons of Pt.

From there we have calculated the interaction of SnPor–Pt with O_2 and water. Our results indicate that the dissociation barrier of O_2 on SnPor–Pt is 1.8 eV. This value is just slightly higher than that of the Pt(111) surface. We are currently completing the reaction path studies for the ORR on SnPor–Pt; so far, the results are promising. Details of these calculations will be discussed in a future paper.

Table 1. Structural parameters and binding energies of MoO(Por) and its dioxygen complexes. The bond lengths are in Å and binding energies in eV. 'Cal' gives the calculated structural parameters in this work and 'Exp' gives the experimental structural parameters obtained by XRD [67, 68]. Mo refers to the molybdenum atom in the centre of the porphyrin ring; N1, N2, N3 and N4 are the nitrogen atoms, and O1, O2, and O3 are the oxygen atoms. The white spheres are the carbon atoms, and the other spheres are the hydrogen atoms. Mo–N_p is the average of the distances between Mo and the planes formed by all three-atom combinations of the four nitrogen atoms N1, N2, N3, and N4.

Complex	MoO(Por)		MoO(Por) (O₂) Side-on		MoO(Por) (O₂) End-on
Structure					
	Cal	Exp [67]	Cal	Exp [68]	Cal
Mo–O1	1.69	1.656(6)	1.71	1.697(13)	1.71
Mo–O2			1.98	1.945(18)	1.98
Mo–O3			1.98	1.948(19)	3.08
Mo–N1	2.14	2.113(9)	2.27	2.256(7)	2.20
Mo–N2	2.14	2.110(11)	2.17	2.116(7)	2.18
Mo–N3	2.14	2.104(9)	2.43	2.320(6)	2.21
Mo–N4	2.14	2.115(10)	2.17	2.121(7)	2.19
Mo–N_p	0.635	0.6389(8)	1.04	1.00	0.86
O2–O3			1.42	1.42(3)	1.32
Binding energy	0.000		0.611		−0.153

Variants of this system, including replacing SnPor with GePor or PbPor [62] and replacing platinum with Ni, Co, Fe and other metals [63], are also being studied. We are also simulating the interaction of SnPor–Pt with H_2O and –OH in an aqueous medium to complete the ORR path to check if the ORR will lead to completion or if it would react too strongly with these species, quickly leading to poisoning of the reactive site.

4.3. Oxomolybdenum porphyrin

It is experimentally known that the O–O bond length increases after O_2 is adsorbed on oxomolybdenum porphyrin, MoO(Por) [64, 65]. We studied the adsorption of O_2 on oxomolybdenum porphyrins by using first-principles calculations considering both side-on and end-on configurations, and how the energy levels of molecular orbitals in oxomolybdenum porphyrin change after the adsorption of O_2 [66]. Table 1 shows structural parameters and binding energies of MoO(Por) and its dioxygen complexes. From the calculated results, it was found that the adsorbed O_2 on MoO(Por) takes a side-on configuration, in agreement with experimental results [67]. The bond lengths of Mo–O_2 and that of Mo–O_3 are completely equal, and both are longer than that of Mo–O_1. Furthermore, the binding energy of the adsorbed O_2 in MoO(Por) is about 0.611 eV, which indicates that the Mo–O_2 bond is weakly stable. This is also supported by the experimental results that demonstrate the reversible dioxygenation behaviour of MoO(Por) (O_2) by photoirradiation or heating [64]. The bond length of the adsorbed O_2 is 1.42 Å, much longer than that of gaseous O_2, 1.2 Å.

By analysing both molecular orbitals and electron densities of MoO(Por) and its side-on dioxygen complex, we found that the electrons in the HOMO, which are mainly made of the

d orbitals of the Mo atom, transfer to the empty π^* orbitals of the incoming O_2 to become more stable, while the electrons in other orbitals stay the same. As an increase in the π^* orbital occupancy and bond lengthening indicates weakening, we think it causes the formation of isolated O atoms for further reaction with protons and electrons to produce the water molecules easier.

We are also simulating the interaction of MoO(Por) with H_2O and –OH in an aqueous medium to complete the reaction path to check if the O_2 reduction reaction will proceed to completion or if it would react too strongly with these species, quickly leading to poisoning of the reactive site.

5. Conclusion

ORR is the bottleneck of a fuel cell's catalytic combustion process even on the widely used Pt surface. Both experimental and DFT studies indicate that haem-based materials have potentials as oxygen reduction catalysts in fuel cells. But more research is required to create a novel material that can rival platinum in terms of efficiency and durability. We have proposed several solutions.

We think that reducing the O–O bond dissociation energy barrier is a first step towards improving ORR catalytic activity. (The O–O activation barrier on the stable Pt(111) surface is 1.7 eV.) Our early studies consider utilizing physical techniques to achieve this—inducing the side-on interaction of O_2 with FePor and inducing the triplet state of FeP-O_2. The O–O bond of the side-on adsorbed O_2 on FePor–O_2 is relatively weak (1.42 Å versus 1.2 Å of O_2 gas in vacuum) and the side-on O–O bond dissociation barrier (1.35 eV) on FePor is energetically comparable to that of the well-known platinum catalyst. It was suggested that singlet O_2 be impinged on haem to dissociate O_2 via the side-on orientation. Another proposal involves magnetizing (Im)FePor–O_2 (FePor–O_2 with an imidazole) to the triplet state. The Im was said to enhance spin polarization on the Fe and weakening of O–O bond in the triplet state. By doing so, the activation barrier for the O–O dissociation barrier is lowered to 1.19 eV. We think that a strong external magnetic field may be applied for this purpose.

While these physical techniques are academically important, they remain challenging tasks. Consequently, our present focus is on designing novel materials by density functional calculations—namely CcO mimics, SnPor–Pt and MoO Por.

For the CcO mimic, we consider FePor and Cu(Im)$_3$ as the representative of the active binuclear centre. The Cu binds to the distal oxygen atom of FePor–O_2. This manifests an increase in O–O bond length (1.32 Å for FeP–O_2 versus 1.38 Å for FeP–O_2–Cu(Im)$_3$) and a decrease in O–O stretching frequency (1211–1082 cm^{-1}). We find that the Cu(Im)$_3$ weakens the O–O bond primarily by electron transfer to the oxygen atoms. O_2 bond weakening leads to easier O–O bond dissociation while the negative charge transfer to O makes it more reactive to H^+; both suggest ORR catalysis.

For SnPor–Pt, we consider depositing Pt directly on SnPor surfaces as a way to minimize the Pt load in catalysts. Our calculations show that Pt can bond strongly on SnPor. The binding energy of platinum on SnPor was 3.13 eV, and the frontier electrons correspond primarily to the valence d-electrons of Pt. Our results indicate that the dissociation barrier of O_2 on SnPor–Pt is 1.8 eV. This value is just slightly higher than that of the Pt(111) surface (1.7 eV).

For MoO(Por), the binding energy of the adsorbed O_2 in MoO(Por) is about 0.611 eV, which indicates that the Mo–O bond is weakly stable. The bond length of the adsorbed O_2 is 1.42 Å, much longer than that of gaseous O_2 (1.2 Å). By analysing both molecular orbitals and electron densities of MoO(Por) and its side-on dioxygen complex, we found that the electrons in the HOMO, which are mainly made of the d orbitals of the Mo atom, transfer to the π^*

orbitals of the incoming O_2 to become more stable, while the electrons in other orbitals stay the same. As an increase in the π^* orbital occupancy and bond lengthening indicates weakening, we think it causes the formation of isolated O atoms for further reaction with protons and electrons to produce the water molecules more easily.

We are simulating the interaction of these designed haem-based materials with H_2O and –OH in an aqueous medium to complete the ORR path to check if the ORR will proceed to completion or if it would react too strongly with these species, quickly leading to poisoning of the reactive site. And by way of this status report, we are also inviting experimentalists to verify our findings.

Acknowledgments

References

[1] Graham A P, Menzel A and Toennies J P 1999 *J. Chem. Phys.* **111** 1676–85
[2] Roman T, Nakanishi H, Diño W A and Kasai H 2006 *e-J. Surf. Sci. Nanotechnol.* **4** 619–23
[3] Wroblowa H, Pan Y C and Razumney G 1976 *J. Electroanal. Chem.* **69** 195–201
[4] Markovic N M and Ross P N 1999 *Interfacial Electrochemistry: Theory, Experiment and Applications* ed A Wieckowski (New York: Dekker) pp 821–41
[5] Markovic N M and Ross P N 2002 *Surf. Sci. Rep.* **45** 117–229
[6] Adzic R 1998 *Electrocatalysis* ed J Lipkowski and P N Ross (New York: Wiley) pp 197–242
[7] Gland J L, Sexton B A and Fisher G B 1980 *Surf. Sci.* **95** 587
[8] Dicke J, Rotermund H H and Lauterbach J 2000 *Surf. Sci.* **454** 352–7 and references quoted therein
[9] Eichler A and Hafner J 1997 *Phys. Rev. Lett.* **79** 4481–4
[10] Yotsuhashi S, Yamada Y, Diño W A, Nakanishi H and Kasai H 2005 *Phys. Rev.* B **72** 033415
[11] Eiswirth M, Möller P, Wetzl K, Imbihl R and Ertl G 1989 *J. Chem. Phys.* **90** 510–21
[12] Cox M P, Ertl G and Imbihl R 1985 *Phys. Rev. Lett.* **54** 1725
[13] Rotermund H H, Engel W, Kordesch M and Ertl G 1990 *Nature* **343** 355
[14] Markovic N, Gasteiger H and Ross P 1997 *J. Electrochem. Soc.* **144** 1591–7
[15] Gojkovic S L and Savinell R F 1997 *J. Electrochem. Soc.* **144** 2973–9
[16] Chen S and Kucernak A 2004 *J. Phys. Chem.* B **108** 3262–76
[17] Paulus UA, Schmidt T J, Gasteiger H A and Behm R J 2001 *J. Electroanal. Chem.* **495** 134–45
[18] Dhanda A, O'Hayre R and Pitsch H 2006 *210th ECS Mtg* Abstract #1958
[19] Ekström H, Hanarp P, Gustavsson M, Fridell E, Lundblad A and Lindbergh G 2006 *J. Electrochem. Soc.* **153** A724–30
[20] Anderson A B and Albu T V 2000 *J. Electrochem. Soc.* **147** 4229–38
[21] Sidik R A and Anderson A B 2002 *J. Electroanal. Chem.* **528** 69–76
[22] Nørskov J K, Rossmeisl J, Logadottir A, Lindqvist L, Kitchin J R, Bligaard T and Jonsson H 2004 *J. Phys. Chem.* B **108** 17886–92
[23] Tsuda M, Diño W A, Nakanishi H and Kasai H 2004 *e-J. Surf. Sci. Nanotechnol.* **2** 226–9
[24] Nakanishi H, Miyamoto K, David M, Dy E, Tanaka R and Kasai H 2007 *J. Phys.: Condens. Matter* at press

[25] Proniewicz L M, Paeng I R and Nakamoto K 1991 *J. Am. Chem. Soc.* **113** 3294–303
[26] Woolery G L, Walters M A, Suslick K S, Powers L S and Spiro T G 1985 *J. Am. Chem. Soc.* **107** 2370–3
[27] Bajdor K, Oshio H and Nakamoto K 1984 *J. Am. Chem. Soc.* **106** 7273–4
[28] Rovira C, Kune K, Hutter J, Ballone P and Parrinello M 1997 *J. Phys. Chem.* A **101** 8914–25
[29] Dawson J H, Holm R H, Trudell J R, Barth G, Linder R E, Bunnenberg E, Djerassi C and Tang S C 1976 *J. Am. Chem. Soc.* **98** 3707–9
[30] Tsuda M, Dy E S and Kasai H 2005 *J. Chem. Phys.* **122** 244719
[31] Collman J P *et al* 1974 *Proc. Natl Acad. Sci. USA* **71** 1326–9
[32] Vogel K M, Kozlowski P M, Zgierski M Z and Spiro T G 1999 *J. Am. Chem. Soc.* **121** 9915–21 and references therein
[33] Rovira C and Parrinello M 2000 *Int. J. Quantum Chem.* **80** 1172–80
[34] Momenteau M and Reed C A 1994 *Chem. Rev.* **94** 659–98
[35] Silaghi-Dumitrescu R 2004 *J. Biol. Inorg. Chem.* **9** 471–6 and references cited therein
[36] Han S, Ching Y-C and Rousseau D L 1990 *Nature* **348** 89–90
[37] Springer B A, Sligar S G, Olson J S and Phillips G N Jr 1994 *Chem. Rev.* **94** 699–714
[38] Spiro T G and Kozlowski P M 2001 *Acc. Chem. Res.* **34** 137
[39] Collman J P, Boulatov R, Sunderland C J and Fu L 2004 *Chem. Rev.* **104** 561–88
[40] Tarasevich M R, Sadkowski A and Yeager E 1983 *Comprehensive Treatise of Electrochemistry* vol 7, ed J O'M Bockris, B E Conway, E Yeager, S U M Khan and R E White (New York: Plenum) pp 301–98
[41] Tanaka A A, Fierro C, Scherson D and Yaeger E B 1987 *J. Phys. Chem.* **91** 3799–807
[42] Lai M E and Bergel A 2000 *J. Electroanal. Chem.* **494** 30–40
[43] Maruyama J and Abe I 2005 *Chem. Mater.* **17** 4660–7
[44] Tsuda M, Dy E S and Kasai H 2006 *Eur. Phys. J.* D **38** 139–41
[45] Aquilanti V, Ascenzi D, Cappelletti D and Pirani F 1994 *Nature* **371** 399–402
[46] Aquilanti V, Ascenzi D, Cappelletti D and Pirani F 1995 *J. Phys. Chem.* **99** 13620–6
[47] Aquilanti V, Bartolomei M, Pirani F, Cappelletti D, Vecchiocattivi F, Simizu Y and Kasai T 2005 *Phys. Chem. Chem. Phys.* **7** 291–300
[48] Tsuda M, Diño W A and Kasai H 2005 *Japan. J. Appl. Phys.* **44** L57–9
[49] Yoshikawa S, Shinzawa-Itoh K, Nakashima R, Yaono R, Yamashita E, Inoue N, Yao M, Fei M J, Libeu C P, Mizushima T, Yamaguchi H, Tomizaki T and Tsukihara T 1998 *Science* **280** 1723–9
[50] Tsuda M, David M and Kasai H 2006 *Surf. Sci.* **600** 3992–4
[51] Collman J P, Devaraj N K, Decréau R A, Yang Y, Yan Y L, Ebina W, Eberspacher T A and Chidsey C E D 2007 *Science* **315** 1565–8 and references quoted therein
[52] Onaka S, Kondo Y, Yamashita M, Tatematsu Y, Kato Y, Goto M and Ito T 1985 *Inorg. Chem.* **24** 1070–6
[53] Barbe J-M, Guilard R, Lecomte C and Gerardin R 1984 *Polyhedron* **3** 889–94
[54] Onaka S, Kondo Y, Toriumi K and Ito T 1980 *Chem. Lett.* 1605–8
[55] Kadish K M, Swistak C, Boisselier-Cocolios B, Barbe J-M and Guilard R 1986 *Inorg. Chem.* **25** 4336–43
[56] Guilard R, Fahim M, Zaegel F, Barbe J-M, d'Souza F, Atmani A, Adamian V A and Kadish K M 1996 *Inorg. Chim. Acta* **252** 375–82
[57] Noda I, Kato S, Mizuta M, Yasuoka N and Kasai N 1979 *Angew. Chem. Int. Edn Engl.* **18** 83
[58] Wang S, Tabata I, Hisada K and Hori T 2002 *Dyes Pigments* **55** 27–33
[59] Wang Z, Medforth C J and Shelnutt J A 2004 *J. Am. Chem. Soc.* **126** 16720–1
[60] Song Y, Steen W A, Peña D, Jiang Y B, Medforth C J, Huo Q, Pincus J L, Qiu Y, Sasaki D Y, Miller J E and Shelnutt J A 2006 *Chem. Mater.* **18** 2335–46
[61] Dy E S and Kasai H 2006 *Chem. Phys. Lett.* **422** 539–42
[62] Dy E S and Kasai H 2007 *J. Phys.: Condens. Matter* accepted
[63] Dy E S and Kasai H 2006 *Eur. Phys. J.* D **41** 241–5
[64] Tachibana J, Imamura T and Sasaki Y 1998 *Bull. Chem. Soc. Japan.* **71** 363–9
[65] Fujihara T, Sasaki Y and Imamura T 1999 *Chem. Lett.* **28** 403–4
[66] Kubota Y, Dy E S, Nakanishi H, Kasai H and Diño W A 2006 *e-J. Surf. Sci. Nanotechnol.* **4** 630–5
[67] Fujihara T, Rees N H, Umakoshi K, Tachibana J, Sasaki Y, McFarlane W and Imamura T 2000 *Chem. Lett.* **29** 102–3
[68] Diebold T, Chevrier B and Weiss R 1979 *Inorg. Chem.* **18** 1193–200